

A study of aging effects of barrel time-of-flight system in the BESIII experiment[☆]

Huan-Huan Liu^{a,b,1}, Sheng-Sen Sun^{a,b,1}, Shuang-Shi Fang^{a,b}, Zhi Wu^{a,c},
Hong-Liang Dai^{a,c}, Yue-Kun Heng^{a,b,c}, Ming Zhou^{a,b}, Zi-Yan Deng^a,
Huai-Min Liu^a

^a*Institute of High Energy Physics, Chinese Academy of Sciences, Beijing 100049, China*

^b*University of Chinese Academy of Sciences, Beijing 100049, China*

^c*State Key Laboratory of Particle Detection and Electronics, Beijing 100049, China*

Abstract

The time-of-flight system consisting of plastic scintillation counters plays an important role for particle identification in the BESIII experiment at the BEPCII double ring e^+e^- collider. Degradation of the detection efficiency of the barrel TOF system has been observed since the start of physical data taking and this effect has triggered intensive and systematic studies of aging effects of the detector. The aging rates of the technical attenuation lengths and relative gains are obtained based on the data acquired in past several years. This study is essential for ensuring an extended operation of the barrel TOF system under the optimal conditions.

Keywords: time-of-flight system, scintillation counter, aging effect, attenuation length;

PACS: 82.80.Rt, 29.40.Mc

[☆]Supported in part by National Natural Science Foundation of China (U1232201, 11575225, 11675184, 11605220), National Key Basic Research Program of China (2015CB856700), the CAS center for Excellence in Particle Physics.

*Corresponding author

Email addresses: hhliu@ihep.ac.cn (Huan-Huan Liu), sunss@ihep.ac.cn (Sheng-Sen Sun)

1. Introduction

The Beijing Spectrometer (BESIII) detector [1] was designed to study physics in the τ -charm energy region at the high luminosity Beijing Electron Positron Collider (BEPCII) [2, 3]. The time-of-flight (TOF) system based on plastic scintillation counters plays a key role for particle identification in the BESIII experiment, especially for K/π separation, it can also provide fast trigger signals. The TOF system consists of a double layer barrel and two single layer end caps [1, 4]. The solid angle coverage of the barrel TOF is $|\cos \theta| < 0.83$, while that of the end cap is $0.85 < |\cos \theta| < 0.95$. The end cap time-of-flight detector was upgraded with multi-gap resistive plate chamber (MRPC) technology in summer of 2015 [5, 6, 7, 8]. In this article, the investigation of the aging effects on the performance of the scintillation counters of the barrel TOF system is described.

The physics data taking of BESIII detector was began in 2009. The detection efficiency of barrel TOF system is found to be decreased with time since then, and no obvious deterioration of time resolution is observed. The time dependence of detection efficiency of electrons or positrons in Bhabha events for a typical scintillation counter of barrel TOF system distribution is shown in Fig. 1. The detection efficiency is defined as $\varepsilon = n_{\Delta t}/n_{track}$, n_{track} is the number of MDC tracks extrapolated to barrel TOF, and $n_{\Delta t}$ is the number of MDC tracks with their time differences between measured and expected times less than a specific value, such as 1 ns, in order to suppress the background. The reduction of the number of output signals from the high threshold discriminators caused by the aging effect of scintillation counters and photomultiplier tubes predominately contributes to the degradation of performance of the TOF detector. The high voltages of PMTs of barrel TOF system were increased twice in 2012 and 2016, the reduced output signals were amplified and the efficiency-drops were recovered.

In view of the importance of particle identification and the maintenance over the whole lifetime of the experiment, the intensive and systematic study of

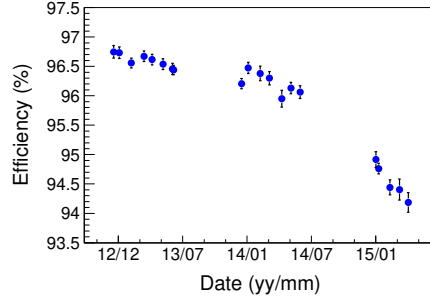


Figure 1: Time dependence of detection efficiency for a typical scintillation counter of barrel TOF system distribution.

aging effects of time-of-flight detector system is essential for making the long-term forecast.

2. The barrel time-of-flight system

The barrel TOF system has two layers of staggered scintillation counters
 35 mounted on the outer surface of the main drift chamber (MDC). Each layer
 has 88 scintillation counters (BC408) [9, 10, 11] read out by fine-mesh photo-
 multiplier tubes (PMT). The scintillator bar cross-section is trapezoidal, and
 the length and thickness are 2300 mm and 50 mm respectively. Two PMTs
 (Hamamatsu R5924) are attached to the two ends of a counter and coupled by
 40 a 1 mm thick silicone pad (BC634A). The length of the PMT is 50mm, and
 the total length of PMT assembly is 103 mm, including the base and preamp.
 The TOF readout system [12] consists of preamplifiers mounted in the PMT
 bases, cables, signal time and amplitude measurement circuits and a laser cal-
 ibration system. A dual threshold discriminator scheme, designed to reduce
 45 noise while maintaining low time walk, is used for time digitization. The out-
 puts from the low threshold discriminators of the two ends are used to start the
 precision time-to-digital conversion (TDC) process and are put into coincidence
 with the high threshold discriminator outputs in order to reduce background
 rates. The signal amplitude measurement circuit is based on the charge-to-time

50 conversion (QTC) principle. A more complete description of the time-of-flight system employed at BESIII, its design and arrangement can be found in the articles [1, 4].

3. Attenuation length measurements

The plastic scintillator utilize the ionization produced by incident charged
 55 particles to generate optical photons. Organic scintillator, including plastic scintillator, does not respond linearly to the ionization density. A semi-empirical model by Birks describes the light-output degradation at high ionization density [13]:

$$\frac{d\mathcal{L}}{dx} = \mathcal{L}_0 \frac{dE/dx}{1 + k_B dE/dx}, \quad (1)$$

where \mathcal{L} is the luminescence, \mathcal{L}_0 is the luminescence at low specific ionization
 60 density, dE/dx is the ionisation energy loss in $MeV/(g/cm^3)$ and k_B is Birks' constant, which is characteristic for the scintillation material. The produced photons are then propagated by total internal reflection, refraction and absorption in the scintillator until they arrive at the PMTs located at the ends of the scintillator and make a signal pulse. This light attenuation is described as an
 65 exponential function with the technical attenuation length λ which is defined as the length reducing the light signal by a factor of e . For the barrel TOF, the measured signal pulse height(charge) QTCs of two ends of a scintillator, q_1 and q_2 could be expressed as:

$$\begin{aligned} q_1 &= A_1 \cdot \frac{q_0}{\sin \theta} \cdot \exp\left(-\frac{l/2 - z}{\lambda}\right), \\ q_2 &= A_2 \cdot \frac{q_0}{\sin \theta} \cdot \exp\left(-\frac{l/2 + z}{\lambda}\right), \end{aligned} \quad (2)$$

where the subscripts 1 and 2 represent the readout channels in the directions
 70 along the positron beam and the opposite, respectively; A_1 and A_2 are the relative gains, including the contributions of light yields of scintillation bars, the quantum efficiencies (QEs), photon-electron collection efficiencies (CEs), multiplication gains of PMTs and preamplifier gains for the two readout channels

respectively; θ is the polar angle of the incident particle with respect to the
75 direction of the positron beam; l is the total length of the scintillator bar; z
is the extrapolated hit position along the scintillator bar based on the particle
trajectory [14]; q_0 is the normalized pulse height at $z = 0$ and $\theta = 90^\circ$, which is
proportional to the luminescence of the vertical incident particle.

From Eq. 2, it is easily to deduce the following equation

$$\ln\left(\frac{q_1}{q_2}\right) = \ln\left(\frac{A_1}{A_2}\right) + \frac{2 \cdot z}{\lambda}. \quad (3)$$

80 The scattering plot of $\ln(q_1/q_2)$ versus hit position z of incident charged particle
is shown in Fig. 2. Technical attenuation length λ and relative gain ratio A_1/A_2
could be extracted through a linear fitting to $\ln(q_1/q_2)$ versus hit position z
using real data. The nonlinearity behavior close to two ends of the scintillator
bar is caused by the saturation of QTC measurements and edge effects.

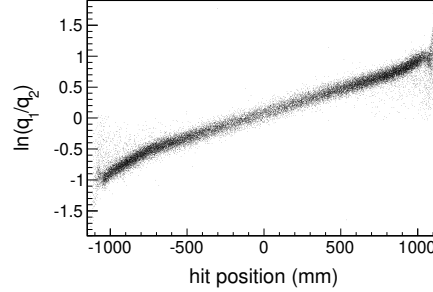


Figure 2: The scattering plot of $\ln(q_1/q_2)$ versus hit position z .

85 The technical attenuation length dependence as a function of time is ex-
pressed as:

$$\lambda(t) = \lambda_0 e^{-\alpha \cdot t}, \quad (4)$$

where λ_0 is the technical attenuation length at the beginning of measurements;
 $\lambda(t)$ is the technical attenuation length at time t ; t is the time; α is the counter
aging constant.

90 Data sample of the electrons and positrons in Bhabha events which is selected
using online event filtering algorithm [15] is employed for the measurements of

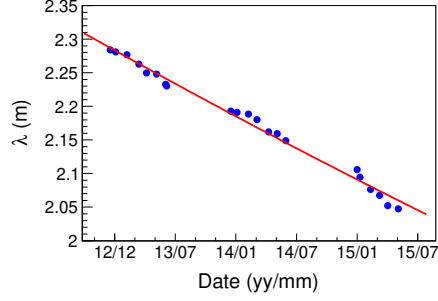


Figure 3: Time dependence of technical attenuation length for a typical scintillation counter of barrel TOF system distribution.

technical attenuation lengths. In the course of several years, the measurements of technical attenuation length of each scintillator counter is performed periodically using the method shown in Eq. 3. The plot of time dependence of the technical attenuation length for a typical scintillation counter of barrel TOF system, together with an exponential function of Eq. 4, is shown in Fig. 3. The aging constant is measured individually for each scintillation counter. The distribution of aging constants is shown in Fig. 4, which is approximately described by a Gaussian function. The average experimental value for aging constant of 176 counters $\alpha = 0.045/\text{year}$, corresponds to degradation annual rate of about 4.4%.

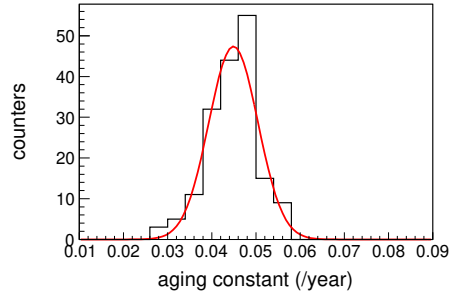


Figure 4: Distribution of the individually calculated aging constant for each scintillation counter together with the Gaussian distribution fitted to the data.

4. Relative gains

From 2012 to 2015, the center-of-mass energies of physics data taking are 2~4.6 GeV, corresponding the $\beta\gamma$ s of electrons and positrons in Bhabha events
105 are around 2000~4600. Since the relativistic rise of the energy loss saturates in this $\beta\gamma$ range described by the “Bethe equations” [16], the differences of mean rate of energy loss per length of Bhabha events taken at different energy points could be negligible. That means, the ideal luminescence intensity or normalized pulse height q_0 of Bhabha events at different energy points would
110 remain the same as a specific constant. As above definition in Eq. 2, the relative gains A_1 and A_2 have contributions of light yield of the same scintillator bar, efficiencies and multiplication gains of PMTs and preamplifier gains for the two readout channels respectively. At present, it is extremely difficult to access the scintillation counters in their positions inside the BESIII detector. Therefore
115 it is impossible to extend the investigation of the aging to a large number of scintillator bars, PMTs and electronics preamplifiers separately. However, since the degradation of measured signal pulse height is expected to be accompanied by the aging effect of relative gains of contributions of each part of this sequential chain, the investigation of aging effect of relative gains is performed instead of
120 separate investigations of aging effects of scintillator bars, PMTs and electronics channels.

The products of relative gains of two ends of one scintillator bar and normalized pulse height could be derived from Eq. 2,

$$\begin{aligned} A_1 \cdot q_0 &= q_1 \cdot \sin \theta \cdot \exp\left(\frac{l/2 - z}{\lambda}\right), \\ A_2 \cdot q_0 &= q_2 \cdot \sin \theta \cdot \exp\left(\frac{l/2 + z}{\lambda}\right). \end{aligned} \quad (5)$$

Using the same data sample of Bhabha events for the study of the attenu-
125 ation length, the distribution of product of relative gain and normalized pulse height of a typical electronics channel is shown in Fig. 5, together with the best approximation using the Landau function [17].

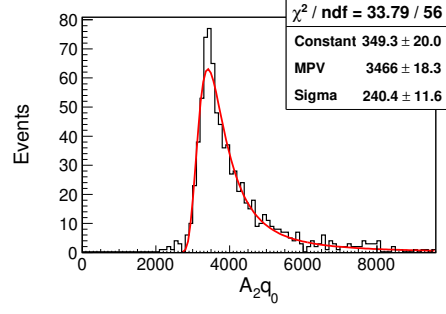


Figure 5: The distribution of product of relative gain and normalized pulse height of a typical electronics channel.

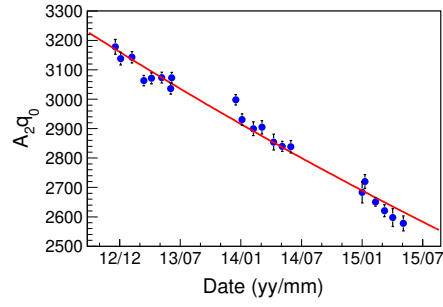


Figure 6: The distribution of time dependence of the most probable value of the product of relative gain and normalized pulse height.

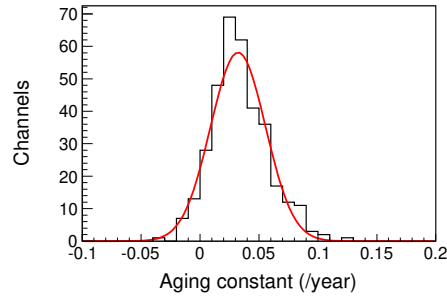


Figure 7: Distribution of the individually calculated aging constant for each readout channel together with a Gaussian fit.

The plot of the time dependence of the most probable value (MPV) of the product of relative gain and normalized pulse height of a typical channel is shown in Fig. 6. Since the ideal normalized pulse height q_0 approximates to a constant without time dependence, almost same exponential function as Eq. 4 is obtained for the result fitting,

$$A(t) = A_0 e^{-\alpha \cdot t} \quad (6)$$

where A_0 is the relative gain at the beginning of measurements; $A(t)$ is the relative gain at time t , t and α are the time and the relative gain aging constant respectively.

For each electronics readout channel, the aging constant of relative gain is obtained with Eq. 6 individually. The distribution of aging constants of relative gains is shown in Fig. 7, and this distribution is fitted using a Gaussian function. The average experimental value for aging constant of relative gains of 352 readout channels, $\alpha = 0.032/\text{year}$, corresponds to degradation annual rate of about 3.2%.

5. Estimation of lifetime of photomultiplier tubes

The BESIII detector is configured around a 1T superconducting solenoid (SSM), considered to be optimum for precise momentum measurements for charged tracks in the $\tau - \textit{charm}$ energy region. And another two superconduction quadrupoles (SCQs) are inserted in the conical shaped MDC end caps as close as possible to the interaction point. Fewer secondary electrons would get to hit the dynodes and resultantly reduce the multiplication gain under a high magnetic field, The fine-mesh PMTs R5924 by Hamamastu have a high resistivity against magnetic field because of its 19 stages of fine-mesh dynodes, which has many apertures to let electrons go through. A fast preamplifier with a gain of 10 is installed in the PMT base to boost signals and extend the lifetime of the PMT.

Since the start of engineering run of BEPCII in collision mode in 2008 to 2015, the total running time is about 15869 hours. The average event rate is

around 300KHz with the event satisfies the TOF trigger condition, number of hits in the barrel TOF is equal to 1 or larger. For each PMT, the average hit rate is about 0.04 per event and the most probable value of charge distribution is about 12pC, these numbers are obtained based on random trigger data sample.

160 The integrated amounts of output charge from a PMT anode is 8.2C totally. This is a conservative estimation since the small signals which could not be over threshold has no record in the raw data. The magnitude of integrated amounts corresponding to 7-year time duration is far smaller than the limit of lifetime of PMT 360C.

165 **6. Summary**

Investigation shows that the degradation of detection efficiency of barrel TOF system is related to the aging effect of the detector, and no significant deterioration of time resolution is observed since the start of physics data taking of BESIII. Therefore we performed a study on the aging rates for technical atten-
 170 uation length and relative gain using the Bhabha event taking in the period of 2012-2015. A brief estimation of the lifetime of the PMTs shows they should be safe under the same irradiation circumstance over the long term. These numbers allow us to forecast the detection efficiency and make an appropriate plan to ensure the detector operation under the optimal conditions. The high voltages
 175 of photomultiplier tubes of the barrel TOF system have been increased twice for the optimal performance of the detector since 2009. The relationship between the multiplication gain and high voltage of PMT could be described using an exponential function and the gain will become saturated with enough high HV. Except increasing the HV of PMTs, decreasing the thresholds of electronics is
 180 another choice for the recovery of the detection efficiency. Some experiments about the tuning of threshold are expected to make the quantitative description available. The relative gain includes the contributions of light yield of scintillator bar, efficiencies and gain of PMT and preamplifier gain of electronics channel. In this study, the aging effect of the relative gain is considered as a

185 whole of these contributions. Individual investigations of aging properties of
 scintillation counters, PMTs and electronics would lead to an improved under-
 standing of aging phenomena and enable to extend the operational period, so a
 further study is still necessary for long term forecast, such as 8-10 years. Thus a
 detailed proposal for studying the light yield of scintillation counter, the quan-
 190 tum efficiency, photon-electron collection efficiency and multiplication gain of
 PMT and preamplifier gain for the readout channel is now in preparation.

References

- [1] BESIII Collaboration (M. Ablikim, et al.), Design and Construction of the
 BESIII Detector, Nucl. Instrum. Meth. **A 614** (2010) 345–399.
- 195 [2] BES Collaboration (J. Z. Bai, et al.), The BES upgrade, Nucl. Instrum.
 Meth. **A 458** (2001) 627–637.
- [3] BESIII Collaboration (M. Ablikim, et al.), Performance of the BEPC and
 progress of the BEPCII, Proceedings of APAC (2004) p. 15–19.
- [4] Y. K. Heng, et al., The Progress of TOF on BESIII, IEEE Nucl. Sci. Symp.
 200 Conf. Rec. (2007) 53–57.
- [5] X. Z. Wang, et al., The cosmic ray test of MRPCs for the BESIII ETOF
 upgrade, Eur. Phys. J. **C 76** (4) (2016) 211.
- [6] X. Z. Wang, et al., The upgrade system of BESIII ETOF with MRPC
 technology, JINST **11** (08) (2016) C08009.
- 205 [7] Zhi Wu, et al. , First results of the new endcap TOF commissioning at
 BESIII, JINST **11** (07) (2016) C07005.
- [8] X. Z. Wang, et al. , BESIII ETOF upgrade readout electronics commis-
 sioning, Chin. Phys. **C 41** (1) (2017) 016103.
- [9] Chong Wu, et al, The timing properties of a plastic time-of-flight scintillator
 210 from a beam test, Nucl. Instrum. Meth. **A 555** (2005) 142–147.

- [10] Z. J. Sun, et al., , High Energy Phys. Nucl. Phys. (in Chinese) **29** (10) (2005) 933–937.
- [11] S. H. An, et al., Testing the time resolution of the BESIII end-cap TOF detectors, Measur. Sci. Tech. **17** (2006) 2650–2654.
- 215 [12] S. B. Liu, C. Q. Feng, Qi An, Y. K. Heng, S. S. Sun, BES III time-of-flight readout system , IEEE Trans. Nucl. Sci. **57** (2010) 419–427.
- [13] J. B. Birks, , Proc. Phys. Soc. **A 64** (1951) 874.
- [14] L. L. Wang, et al., , High Energy Phys. Nucl. Phys. (in Chinese) **31** (2007) 183–188.
- 220 [15] C. D. Fu, et al., Study of the online event filtering algorithm for BESIII, Chin. Phys. **C 32** (2008) 329–337.
- [16] Particle Data Group (K. A. Olive, et al.), Review of Particle Properties, Chin. Phys. **C 38** (2014) 398–412.
- [17] L. Landau, On the energy loss of fast particles by ionization, J. Phys. (USSR) **8** (1944) 201–205.
- 225